

# HALO OCCUPATION DISTRIBUTIONS OF MODERATE X-RAY AGNS THROUGH MAJOR AND MINOR MERGERS IN A $\Lambda$ -CDM COSMOLOGY

L. Altamirano-Dévora, T. Miyaji, H. Aceves, A. Castro, R. Cañas, and F. Tamayo

Instituto de Astronomía, Universidad Nacional Autónoma de México, Ensenada, Baja California, México

*Received ; accepted*

## RESUMEN

Motivados por la forma inferida de la Distribución de Ocupación de Halos (HOD) de Núcleos Activos de Galaxias (AGNs), seleccionados de rayos X en el campo de COSMOS por Allevato et al. (2012), investigamos la HOD de Núcleos Activos de Galaxias de rayos X moderados (mXAGNs) usando un modelo basado en actividad por fusión entre halos de materia oscura (DMHs) en una cosmología  $\Lambda$ CDM. La HOD y las densidades numéricas de los mXAGNs simulados en  $z = 0.5$ , en los escenarios anteriores son calculados y comparados con los resultados de Allevato et al. (2012). Encontramos un comportamiento similar entre las HODs simuladas de fusiones mayores y menores, y la observada para los mXAGNs. El resultado principal es que las fusiones menores, contrario a lo que se podría esperar, pueden jugar un papel importante en activar los mAGNs.

## ABSTRACT

Motivated by recent inferred form of the halo occupation distribution (HOD) of X-ray selected AGNs, in the COSMOS field by Allevato et al. (2012), we investigate the HOD properties of moderate X-ray luminosity Active Galactic Nuclei (mXAGNs) using a simple model based on merging activity between dark matter halos (DMHs) in a  $\Lambda$ CDM cosmology. The HODs and number densities of the simulated mXAGNs at  $z = 0.5$ , under the above scenarios to compare with Allevato et al. (2012) results. We find that the simulated HODs of major and minor mergers, and the observed for mXAGNs are consistent among them. Our main result is that minor mergers, contrary to what one might expect, can play an important role in activity mAGNs.

*Key Words:* Galaxies: active — Methods: numerical, semi-analytical, N-body simulations

## 1. INTRODUCTION

Studies of AGN host galaxies are fundamental to understand the physical mechanisms that trigger AGN activity and govern the fuelling rate of the central black hole (e.g., Gilmour et al. 2009; Alexander & Hickox 2012; Beckmann & Shrader 2012).

The observed correlation between the mass of the central BH and the velocity dispersion ( $\sigma$ ) of the bulge of the host galaxy suggest a strong connection between galaxy evolution and BH activity (e.g., Gebhardt et al. 2000; Merritt & Ferrarese 2001; Tremaine et al. 2002; Kormendy & Ho 2013). This activity is related to the accretion of material to the central engine triggered by, for example: the

merger of gas-rich galaxies (e.g., Silk & Rees 1998; Springel et al. 2005b; Hopkins et al. 2008), bar-driven inflows (e.g., Jogee 2006), disk-instabilities (Bournaud et al. 2011), collisions with molecular clouds (Hopkins & Hernquist 2006), stellar winds from evolved stars (Ciotti & Ostriker 2007), and the transportation of gas to the centers by supernova explosions (Chen et al. 2009) or a combination of these effects.

Mergers and strong interactions can induce substantial gravitational torques on the gas content of a galaxy, depriving it of its angular momentum, leading to inflows and the buildup of huge reservoirs of gas in its center (e.g., Hernquist 1989; Barnes & Hernquist 1991, 1996; Mihos & Hernquist

1996; Springel et al. 2005b; Cox et al. 2006, 2008; Di Matteo et al. 2007). Major galaxy mergers are very efficient in moving gas to galaxy centers due to the generation of large torques. Observationally, visual inspections of host galaxies of AGNs (Treister et al. 2012) find that the more luminous AGNs show recent merger features, while such features are not commonly seen in the less luminous AGNs, which appear to be driven by another process. Low luminosity AGNs could be triggered also in non-merger scenarios (e.g., Milosavljević et al. 2006; Hopkins & Hernquist 2006, 2009), and probably also by the interaction with very small satellites (total mass ratio of about 1:100) as recently suggested (Ramón-Fox & Aceves 2014).

The dominant process that triggers AGN activity could be a function of redshift and/or halo mass. The anti-hierarchical evolution of AGNs (or AGN down sizing), where the number density of low luminosity AGNs comes later in the universe than high luminosity ones (Ueda et al. 2003; Hasinger et al. 2005; Ueda et al. 2014), is probably not consistent with the theoretical predictions of a major merger AGN triggering scenario as suggested by Wyithe & Loeb (2003). Some recent theoretical studies based on cosmological simulations suggest the necessity of a combination of merger and secular processes (e.g., Draper & Ballantyne 2012) or hot-halo accretion and star-burst induced triggering (Fanidakis et al. 2012) to explain the evolution of the luminosity function of AGNs and even their clustering properties (Fanidakis et al. 2013). These results suggest that one or more mechanisms other than major mergers are at least partially responsible for triggering the AGN activity.

Large scale AGN bias measurements show that mXAGNs are on average associated with more massive DMHs than more luminous QSOs (e.g., Miyaji et al. 2007; Krumpel et al. 2010; Allevato et al. 2011). While the typical masses of DMHs associated with QSOs [ $M_{\text{DMH}} \sim 10^{12-13} h^{-1} M_{\odot}$ ; Porciani et al. (2004); Croom et al. (2005); Hopkins et al. (2007); Coil et al. (2007); da Ângela et al. (2008); Mountrichas et al. (2009)] are consistent with a major merger triggering scenario (e.g., Shen 2009), those associated with mXAGNs are typically more massive with  $M_{\text{DMH}} \sim 10^{13-14} h^{-1} M_{\odot}$  (i.e., the mass scale of rich groups-poor clusters). While results from Allevato et al. (2011) suggest that secular processes could trigger mXAGNs.

Cosmological simulations provide an important tool to understand the dark matter distribution in

the universe, the co-evolution and growth of BHs with respect to their host galaxies (e.g., Sijacki et al. 2007; Di Matteo et al. 2008; Thacker et al. 2006). In  $N$ -body simulations the requirement of relating the dark matter to galaxy distributions has to be satisfied (e.g., Pujol & Gaztañaga 2014). Studies of AGN clustering using cosmological simulations have been carried out using the halo model (e.g., Thacker et al. 2009; Degraf et al. 2011) or with the BH continuity equation approach (e.g., Lidz et al. 2006; Bonoli et al. 2009; Shankar et al. 2010). The HOD method allows us to distinguish among AGN evolution models (e.g., Chatterjee et al. 2012). It has been used by several authors to interpret AGN and quasar clustering measurements from direct counts of AGNs within groups of galaxies (e.g., Wake et al. 2008; Shen et al. 2010; Miyaji et al. 2011; Starikova et al. 2011; Krumpel et al. 2012; Allevato et al. 2012; Richardson et al. 2012; Kayo & Oguri 2012; Chatterjee et al. 2013; Krumpel et al. 2014).

The environment of AGN, and in particular the mass of the typical DMHs in which they live, is a powerful diagnostic of the physics that drive the formation of super massive black holes (SMBHs) and their hosts galaxies (e.g., Mountrichas & Georgakakis 2012). By modeling the mean AGN occupation at  $z = 0.5$ , Allevato et al. (2012) found that the host halos of these AGNs have a DMH with mass  $M_{\text{DMH}} \geq 10^{12.75} h^{-1} M_{\odot}$ , that it is a DMH mass for galaxy groups (Eke et al. 2004). This result agrees with studies from Georgakakis et al. (2008) and Arnold et al. (2009) that present evidence that AGNs at  $z \approx 1$  are frequently found in groups. On other hand, Miyaji et al. (2011) calculated the shape of the HOD of X-ray selected AGN that suggests that the AGN satellite fraction increases slowly with  $M_{\text{DMH}}$ , in contrast with the satellite's HOD of low luminosity-limited samples of galaxies. For the latter galaxies, Allevato et al. (2012) found that the slope  $\alpha$  of the HOD distribution of satellite AGNs had a value of  $\alpha_s \leq 0.6$  in their analysis, suggesting a picture in which the average number of satellite AGNs per halo mass decreases with halo mass.

Considering that  $\alpha \approx 1$  is inferred for galaxies in general (e.g., Coil et al. 2009; Zehavi et al. 2011), the HOD studies of AGNs suggest that AGN fraction among galaxies decreases with increasing the DMH mass. The reason for this may be that the cross-section of merging between two galaxies decreases with increasing relative velocity and thus merging frequency is suppressed in a group/cluster environ-

ment with high velocity dispersion (Makino & Hut 1997). Also gas processes such as ram pressure stripping of cold gas in galaxies by hot intra-group/intracluster gas suppresses star formation activities that may feed AGN (Gunn & Gott 1972).

In this work we investigate a scenario where satellite subhalos, from  $N$ -body cosmological simulations harbor mXAGNs within a group/cluster sized parent halo of  $M_{\text{DMH}} \geq 10^{12.75} h^{-1} M_{\odot}$  and have been triggered by either a major or minor merger. We compute the HOD of the simulated mXAGNs and compare them with the inferred HOD obtained by Allevato et al. (2012) and Miyaji et al. (2015) in order to see if we can reproduce such results by using this approach. In general we use a simple approach for coupling cosmological simulations  $\Lambda$ CDM with semi-analytical results to determine the HOD of our numerical AGNs.

The outline of the paper is as follows. In §2 we describe the method used in this work to determine AGN candidates in cosmological simulations to calculate their HOD. In §3 we show our results, discuss them in §4, and finally in §5 we indicate our main conclusions. Throughout this paper we adopt a matter density  $\Omega_{\text{m}} = 0.266$ , dark energy density  $\Omega_{\Lambda} = 0.734$ ,  $H_0 = 72 \text{ km s}^{-1} \text{ Mpc}^{-1}$  and mass RMS fluctuation  $\sigma_8 = 0.816$  consistent with the WMAP7 results of Larson et al. (2011).

## 2. MODEL

In this section we describe the cosmological simulations used and semi-analytical procedure to relate the sub-halo satellites to observational properties of mXAGNs, then the criteria to determine when the merger occurs, and the actual computation of the HOD are described.

### 2.1. Numerical Simulations

A set of five similar  $N$ -body cosmological simulations within the  $\Lambda$ CDM model, each differing from the others in the random seed used to generate the initial conditions were performed.

Each simulation box has a co-moving length of  $L = 100 h^{-1} \text{ Mpc}$  with  $N_{\text{p}} = 512^3$  dark matter particles, each having a mass of  $m_{\text{p}} = 6 \times 10^8 h^{-1} M_{\odot}$ . Initial conditions were generated using 2nd-order Lagrangian Perturbation Theory (e.g., Crocce et al. 2006) starting at a redshift of  $z = 50$ . The initial linear power spectrum density was obtained from the cosmic microwave background code CAMB (Lewis et al. 2000).

The  $N$ -body simulations were carried out using the publicly available parallel Tree-PM code GADGET2 (Springel 2005). The simulations were run

with a softening length of  $\varepsilon = 20 h^{-1} \text{ kpc}$ . Two cosmological simulations were resimulated with  $\varepsilon = 1 h^{-1} \text{ kpc}$  and no change in the HOD results was noted. The change in  $\varepsilon$  can affect the properties of the inner profiles of halos, but that is out of the scope of the present paper.

### 2.2. Halo Finder Algorithm

We identified DMHs and subhalos with the Amiga Halo Finder (AHF) code, which locates halo centers using an adaptive mesh refinement (AMR) approach. In brief, this code finds perspective halo centers, collects particles possibly bound to center, removes unbound particles and calculates halo properties (Knollmann & Knebe 2009; Knebe et al. 2011)<sup>1</sup>. Virial masses are defined using an overdensity of  $200\rho_{\text{c}}$ , where  $\rho_{\text{c}}$  is the critical density of the universe. We used a minimum number of particles  $N_{\text{p}} = 100$  to define a bound halo.

As mentioned in §1, we are interested in DMH with a virial mass of  $M_{\text{DMH}} \geq 10^{12.75} h^{-1} M_{\odot} \equiv M_{\text{th}}$  at  $z = 0.5$  snapshot, in which mXAGN preferentially reside (Allevato et al. 2012; Padmanabhan et al. 2009). This is consistent with the HOD modeling of cross-correlation function between ROSAT all-sky Survey AGNs and luminosity red galaxies (Miyaji et al. 2011). In addition, we focus our attention to those that reside at a non-central location of the host halo.

Halos with  $M_{\text{DMH}} > M_{\text{th}}$  at redshift  $z = 0.5$  are called Host-Halos (HHs hereafter). We then identified subhalos that belong to these HHs, and selected the subhalos that are satellites (Subhalo-Host, SH), see Figure 1.

### 2.3. Connection subhalo to mXAGN

Several approximate methods to assign AGN or quasar activity to halos are described in the literature. For example, Croton (2009) uses the  $M_{\text{BH}}-\sigma$  relation by requiring to reproduce the observed luminosity function of quasars, using the abundance matching technique to “turn-on” halos in the *Millennium* simulation (Springel et al. 2005a). Conroy & White (2013) invoked a model in quasars are treated as a light bulbs, through a empirical model for the demographics and  $M_{\text{BH}}-M_{\text{gal}}$  to match the luminosity function of quasars.

In this section we explain the different scaling relations used in our analysis, in order to relate the subhalos with observational properties of AGNs.

<sup>1</sup><http://popia.ft.uam.es/AHF/Download.html>

### 2.3.1. Black Hole Mass

The central velocity dispersion  $\sigma$  of each SH is related to the black hole mass  $M_{\text{BH}}$  (Kormendy & Ho 2013) by:

$$\log\left(\frac{M_{\text{BH}}}{M_{\odot}}\right) = -0.50 + 4.38 \log\left(\frac{\sigma}{\sigma_0}\right), \quad (1)$$

where  $M_0 = 10^9 h^{-1} M_{\odot}$  and  $\sigma_0 = 200 \text{ km s}^{-1}$ .

### 2.3.2. Assigning Eddington ratio

Given a  $M_{\text{BH}}$ , an Eddington ratio ( $\lambda_{\text{Edd}}$ ) can be defined as:

$$\lambda_{\text{Edd}} = \frac{L_{\text{bol}}}{L_{\text{Edd}}(M_{\text{BH}})} \quad (2)$$

where  $L_{\text{bol}}$  is the bolometric luminosity and  $L_{\text{Edd}}(M_{\text{BH}})$  is the Eddington luminosity, which is proportional to  $M_{\text{BH}}$ .

Combining equation 2 with the data provided in Table 2 of Lusso et al. (2012), we can get the X-ray luminosity as:

$$\log[L_{\text{bol}}/L_{\text{band}}] = a_1 x + a_2 x^2 + a_3 x^3 + b, \quad (3)$$

where  $L_{\text{band}}$  correspond to the 0.5-2 keV band luminosity,  $x = \log L_{\text{bol}} - 12$ ,  $a_1$ ,  $a_2$ ,  $a_3$  and  $b$  are bolometric correction coefficients.

We need to mimic a population of AGNs that represent mXAGNs within our simulations and construct the HOD to compare with the observed mXAGNs HOD by Allevato et al. (2012). To do this we used a representative value of  $\lambda_{\text{Edd}}=0.1$ ,  $a_1=0.248$ ,  $a_2=0.061$ ,  $a_3=-0.041$  and  $b=1.431$ , restricting only subhalos with  $L_x \geq 10^{42.4} h^{-2} \text{ erg s}^{-1}$ .

Using equations (1-3), we obtain the black hole mass threshold  $M_{\bullet}$ , which we use to obtain the number density of subhalos with black holes that can be active or dormant,  $n_{(\geq M_{\bullet})}$ . We also consider a  $z = 0.5$  snapshot, which is the median redshift of the sample used by Allevato et al. (2012). We will assign them to be active or dormant depending on whether they had suffered a galaxy merger within the AGN lifetime  $\tau_{\text{AGN}}$  in the past.

### 2.4. Assigning AGN Lifetime

Instead of using the abundance matching technique, we select the duty cycle (e.g., Cappelluti et al. 2012) as an indicator that the sub-halo was turn on. In the following, we take a simple approach and assume that all AGNs observed at  $z = 0.5$  above the

luminosity threshold, are shining at  $\lambda_{\text{Edd}} = 0.1$  during their lifetime of  $\tau_{\text{AGN}}$ .

Using the X-ray [2–10 keV] band luminosity function (XLF) of AGNs by Miyaji et al. (2015) and the model of the distribution function of the absorbing column density used in Ueda et al. (2014), in combination with the results of Allevato et al. (2012), we estimate the number density of AGNs including absorbed (within Compton-thin range, i.e.,  $N_{\text{H}} < 10^{24} [\text{cm}^{-2}]$ ) and the un-absorbed ones, above the intrinsic (i.e., before absorption) [0.5–2 keV] band luminosity of  $L_x \geq 10^{42.4} h^{-2} \text{ erg s}^{-1}$ . We obtain:

$$n_{\text{AGN}} \sim 4.2 \times 10^{-5} h^3 \text{ Mpc}^{-3}. \quad (4)$$

The idea behind using the 2-10 keV luminosity function is that, the 0.5-2 keV sample used by Allevato et al. (2012) is highly selected against absorbed AGN. In order to estimate a more accurate AGN lifetime, we require a number density of both absorbed and un-absorbed AGNs. Here, for simplicity, we assume that the satellite HODs of absorbed and un-absorbed mXAGNs have the same shape.

To constrain the number density of AGNs that we can observe at  $z = 0.5$  we have used the timescale  $\tau_{\text{AGN}}$ , that indicates when the mXAGNs were activated. We estimate the AGN lifetime  $\tau_{\text{AGN}}$  as follows:

$$\tau_{\text{AGN}} \approx \frac{n_{\text{AGN}}}{n_{(\geq M_{\bullet})}} \times \tau_{\text{age}(z=0.5)}, \quad (5)$$

where  $n_{\text{AGN}}$  is the observed number density of Xray AGNs,  $n_{(\geq M_{\bullet})}$  is the simulated number of SHs with BH mass threshold (active or dormant), and  $\tau_{\text{age}(z=0.5)}$  is the age of the universe at  $z = 0.5$ .

### 2.5. Major and Minor Merger Criteria

We identify major and minor mergers at the redshift corresponding to the AGN lifetime  $\tau_{\text{AGN}}$  before  $z = 0.5$ , so that the triggered AGNs by the mergers during this interval are still active at  $z = 0.5$  under these scenarios.

We define a mass ratio  $\mu = M_2/M_1$  of the progenitors, where  $M_2 > M_1$ . We consider those mergers with the mass ratios  $0.25 \leq \mu \leq 1.0$  as major and those with  $0.1 \leq \mu < 0.25$  as minor mergers, respectively. In order to signal the merger event between two progenitors the following criteria between them have to be satisfied (e.g., Farouki & Shapiro 1981):

1. Their relative velocity  $V_{12} = |V_1 - V_2|$  is less than average of velocity dispersion RMS of both halos ( $V_{\text{rms}}$ ); i.e.,  $V_{12} \leq \langle V_{\text{rms}} \rangle$ .
2. Their relative physical separation  $R_{12} = |r_1 - r_2|$  is less than the sum of the virial radius of both halos:  $R_{12} \leq R_{v1} + R_{v2}$ .

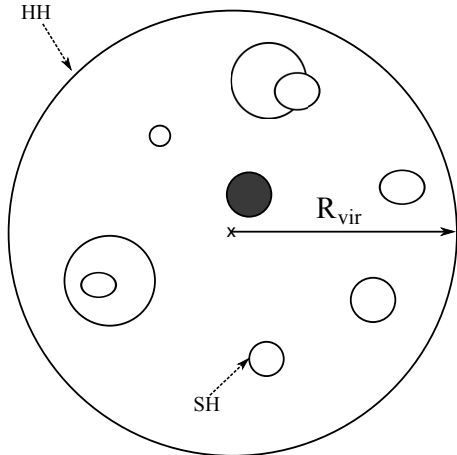


Fig. 1. Schematic diagram illustrates the Host–Halo (HH of mass  $M_{\text{th}}$ ) as circle with virial radius;  $R_v$ . Several subhalos (SHs) are depicted inside  $R_v$ . The central subhalo is identified as the closest to the center of the Host-Halo (dark filled circle) and the others are considered satellite subhalos (empty circles).

To find these merger candidates, we used the **MergerTree** tool which is included in the AHF software, we tag as progenitor the halo which contains the greatest fraction of SH particles (Libeskind et al. 2010). After this initial merging signaling, we verified by inspection of the snapshots that a merger event occurred.

### 2.6. Simulated HOD

The following formula is used in order to compute the HOD of mXAGNs:

$$N(M_{\text{th}}) = \frac{n_{\text{HH}_{\text{agn}}}}{n_{\text{HH}}}, \quad (6)$$

where  $n_{\text{HH}_{\text{agn}}}$  is the number density of HHs that have a SH that has suffered a major or minor merger and has a  $M_{\text{BH}} \geq M_{\bullet}$ , and  $n_{\text{HH}}$  is the total number density of HH (defined in § 2.2) in simulations. The mass bin size used was  $\Delta \log M_{\text{th}}$  is 0.4.

## 3. RESULTS

Before presenting our results we make note of the following. The HOD of Allevato et al. (2012) was evaluated at  $z = 0$ , and their HOD measurement made over a sample extending up to  $z \sim 1$  that was corrected for the 0.5–2 keV XLF and its luminosity-dependent evolution, as indicated by Ebrero et al. (2009). Their sample itself is more representative of  $z \sim 0.5$  than  $z \sim 0$ .

To compare with our results, we back-correct their HOD to  $z \sim 0.5$  in the following way. The Luminosity-Dependent Density Evolution (LDDE)

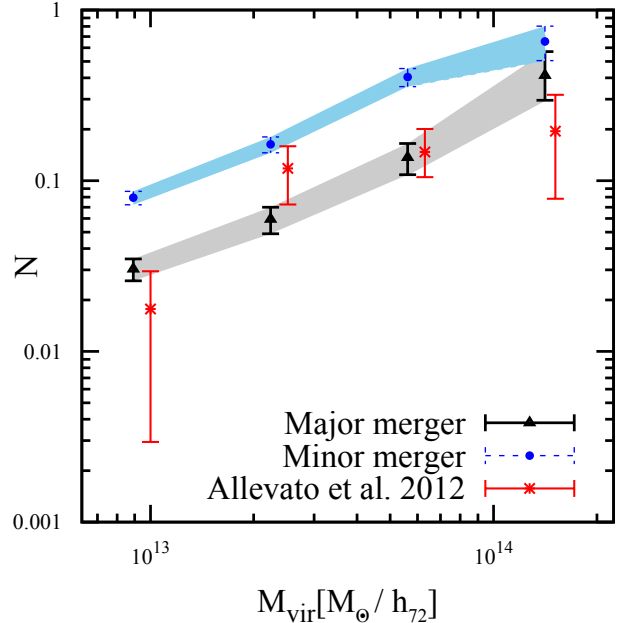


Fig. 2. The HOD of the number of host that harbor a mXAGN triggered by either a major (blue dots) or minor merger (black triangles), and the inferred HOD of satellites mXAGNs by Allevato et al. (2012) (red asterisks). The latter corrected by an evolution factor and adding the un-absorbed AGN estimation of Miyaji et al. (2015). Error bands are calculated as indicated in the text.

model, describing the 0.5–2 keV XLF derived by Ebrero et al. (2009), indicates that the number density grows as  $\propto (1+z)^{3.38}$  up to  $z \sim 0.8$  at all luminosities. Thus, we convert the  $z = 0$  HOD to  $z = 0.5$  HOD results by multiplying by  $(1+0.5)^{3.38} = 3.9$  at all DMH masses. Furthermore, since the Allevato et al. (2012) sample in the 0.5–2 keV band is highly selected against obscured AGNs, we further multiply the HOD by a factor of 2 to account for the obscured AGN contribution using the recent 2–10 keV XLF model by Miyaji et al. (2015). In Figure 2, we plot our results for major and minor mergers HOD and the corrected form of HOD to a redshift of  $z = 0.5$ .

The slope of the HOD shows the same trend for both minor and major mergers for masses  $\lesssim 5 \times 10^{13} h^{-1} M_{\odot}$ . However, at higher masses the minor and major HODs display a somewhat different behavior; with the major merger HOD increasing and the minor one tending to be flat (see Figure 2). To compare with the slope ( $\alpha_s$ ) found by Allevato et al. (2012), we use the same model of occupation function, which is described by:

$$\langle N_{\text{sat}} \rangle (M_h) = f'_a \left( \frac{M_h}{M_1} \right)^{\alpha_s} \exp(-M_{\text{cut}}/M_h); \quad (7)$$

TABLE 1  
NUMBER DENSITIES AND HOD SLOPES

Mechanism	$n_{\text{agn}}$	$\alpha_s$
Major	$2.28 \times 10^{-5}$	$0.20 \pm 0.18$
Minor	$5.96 \times 10^{-5}$	$0.10 \pm 0.09$
Observed <sup>1</sup>	$4.2 \times 10^{-5}$	$0.22^{+0.41}_{-0.29}$

<sup>1</sup>Allevato et al. (2012)

where  $f'_a$  is a normalization,  $M_1$  is the halo mass at which the number of central AGN is equal to that of satellite AGNs ( $\log M_1 = 13.8 M_\odot$ ) and  $M_{\text{cut}}$  is a cut-off mass scale ( $\log M_{\text{cut}} = 13.4 M_\odot$ ).

The fitted slope for the minor merger case was  $\alpha_s = 0.10 \pm 0.09$  and  $\alpha_s = 0.20 \pm 0.18$  for the major merger, which can both be compared with the observed slope obtained by Allevato et al. (2012)  $\alpha_s \leq 0.6$  (Table 1). The slope of minor merger HOD is closer to that of the mXAGN HOD than that of the major merger case. However, both slopes are consistent with the observations.

Errors in Figure 2 were derived as follows. If  $n_{\text{HHagn}}$  is less than 15, we calculate  $1\sigma$  errors using equations (7) & (12) of Gehrels (1986). If  $n_{\text{HHagn}} \geq 15$ , we calculate the  $1\sigma$  errors by  $\sqrt{n_{\text{HHagn}}}$ .

#### 4. DISCUSSION

Different numerical works have addressed the triggering of AGNs, in particular through mergers between galaxies since is a naturally expected contributing process (e.g., Sanders et al. 1988; Hopkins et al. 2006). Major mergers are considered to activate QSO's, a situation that has been studied through hydrodynamical cosmological simulations, the measurements of their clustering and the properties of the AGNs (Sijacki et al. 2007; Di Matteo et al. 2008; Marulli et al. 2009; Ciotti et al. 2010; Degraf et al. 2011; Chatterjee et al. 2012; Van Wassenhove et al. 2012; Krumpe et al. 2015).

However, Schawinski et al. (2011) found that most of the quasars in their sample have disk-like morphologies, suggesting that a secular evolution mechanism can drive the activity to this type of AGNs. Moreover, if only major mergers came to be important at high redshifts the AGNs should probably reside in more elliptical shaped galaxies (Cisternas et al. 2011). In contrast, Lee et al. (2012) and Cisternas et al. (2013) found that the gas bar-driven and the gas that could trigger nuclear activity do not correlate; a mechanism discussed in particular by Wyse (2004).

Stochastic accretion models have been thought to be the triggering mechanism of low/moderate AGN

(Hopkins & Hernquist 2006; Hopkins et al. 2014; Kocevski et al. 2012). Therefore, secular evolution (e.g., Ehlert et al. 2015) came to be an important scenario as well as minor mergers (De Robertis et al. 1998; Hernquist & Mihos 1995; Taniguchi 1999; Kendall et al. 2003; Hopkins & Hernquist 2009; Karouzos et al. 2014), owing to the fact that injection of gas is recurrent and keeps the accretion continuous, that can explain the no-disk AGNs and can influence in some cases the growth of SMBH (e.g., Kaviraj 2014). Considering that intermediate mergers are more common than major mergers (e.g., Tapia et al. 2014), these may also play a role. Recognizing the dominant triggering mechanism is not obvious in all types of AGNs, hence, we made a study in which mXAGNs are triggered by either major and minor mergers using a the HOD formalism and a simplified model.

The accurate time of the merger is difficult to calculate, and therefore the time when the BH will be activated. If we use the dynamical friction time (e.g., Hopkins et al. 2010) to estimate when the progenitors merge, we obtain an important overestimation in comparison to when we follow as closely as we can in time the evolution of the subhalos in our cosmological simulations. Furthermore, results by Jiang et al. (2014) show that is not adequate to take a single timescale to infer when the merging takes place.

In spite of the wide range of probable environments where AGN's live (Villaruel & Korn 2014; Karouzos et al. 2014; Leauthaud et al. 2015), in this work, we are assuming that the host/environment of the mXAGN have a group-like halo mass as indicated by some observations (e.g., Allevato et al. 2012; Silverman et al. 2014). We concentrated our attention in the mXAGNs that reside in non-central subhalos. The connection between galaxies and DMHs has been related in different ways: assigning the stellar mass of the galaxies to DMHs (Degraf et al. 2011; Behroozi et al. 2013), introducing a gas fraction of galaxies into the DMHs (Hopkins et al. 2010; Zavala et al. 2012) and using the luminosity function (Croton 2009). Here we used a combination of semi-empirical and semi-analytic models to seed a black hole in a subhalo/satellite employing the relation  $\sigma - M_{\text{BH}}$ .

The number densities of AGNs in group/cluster can help establish on firmer grounds whether there is any relation between environment density and AGN luminosity (Karouzos et al. 2014), or even, the possible two-phase evolution in X-ray AGNs (Miyaji et al. 2015). It is shown in Figure 2 that the selection of

TABLE 2  
 $\lambda_{\text{EDD}}$  AND  $\alpha_s$

Lambda	Major	Minor
0.01	1.19 $\pm$ 0.16	0.18 $\pm$ 0.04
0.03	0.81 $\pm$ 0.19	0.11 $\pm$ 0.06
0.30	0.54 $\pm$ 0.20	0.15 $\pm$ 0.10

satellite subhalos have a similar distribution in the two merger scenarios tested, i.e., the shape of the HOD can be described to a good extent by both types of mergers. These processes also reproduce approximately the observed number densities of mXAGNs. The results shown in Figure 2 indicate that minor mergers definitively play a role in establishing the HOD of these AGNs, and pin point to the necessity of further research along this line for igniting AGNs.

While we choose to use  $\lambda_{\text{Edd}}=0.1$  from the median value of the  $\lambda_{\text{Edd}}$  distribution from Lusso et al. (2012), it is instructive to show how results change with  $\lambda_{\text{Edd}}$ . Therefore we also computed simulated HODs for  $\lambda_{\text{Edd}} = 0.01, 0.03$  &  $0.3$ . The results are shown in Figure 3 and  $\alpha_s$  values are shown in Table 2. Figure 3 and Table 2 show that the slopes are consistently flat for the minor merger case ( $\alpha_s \approx 0.1 - 0.2$ ) for all  $\lambda_{\text{Edd}}$  values, which are consistent with that of Alleinato et al. (2012). For the major mergers, the slope becomes steep ( $\alpha_s \approx 1$  for  $\lambda_{\text{Edd}} = 0.01$ ), while it is flat for larger  $\lambda_{\text{Edd}}$  values. The global normalization of the minor merger HOD seems to match better with the observation for  $\lambda_{\text{Edd}} = 0.01$  than higher  $\lambda_{\text{Edd}}$  values. However, we note that the normalization is directly proportional to the AGN lifetime  $\tau_{\text{AGN}}$  calculated from Eq. 5, which is a rough approximation. Thus the agreement/disagreement of the HOD normalization between the models and the observation at a level of a factor of a few should not be used to prefer one model from another.

## 5. CONCLUSIONS

In this work, we have used cosmological simulations and semi-analytical methods to assign activity to sub-halo satellites within halos with mass  $M_{\text{th}} \geq 10^{12.75} h^{-1} M_{\odot}$ , and using the merger-driven scenario to trigger the BHs, to obtain an estimate of major and minor mergers contribution to the inferred shape of HOD of mXAGNs.

Testing different models can help to constrain the connection between the AGN and the host galaxy as well as the mechanism that triggers its BH. We have used an estimate of the duty cycle to relate the number density obtained from the simulate mXAGNs to the observed one. Our results bring forward the hy-

pothesis that minor mergers, typically not considered as triggering events, can be an important factor in activating mXAGNs.

Our work shows that the HODs of mXAGNs under major merger and minor merger activation mode are very similar and both are consistent, in our approximate treatment, with the flat slope ( $\alpha_s < 1$ ) inferred from observations. The minor merger model reproduces the slope of the satellite HOD of mXAGNs even at  $\lambda_{\text{Edd}}=0.01$ , while that of the major merger model has a steeper slope at this low  $\lambda_{\text{Edd}}$ .

On other hand, since our simulations do not take into account any baryonic processes, other mechanisms such as the ram-pressure stripping of cold gas is not excluded as a significant cause of the flat slope of the HOD. Our results, however, shows that non-baryonic processes such as the decrease of merging cross section in the high velocity encounters (Makino & Hut 1997), at least be able to produce a flat slope of satellite HOD.

With help of large X-ray surveys like eROSITA and larger samples of mXAGNs in group/cluster we will be able to constrain the properties of the host of these mXAGNs (e.g., mass), and more sophisticated models can lead us to get a better understanding of co-evolution of the AGNs and its distribution.

## Acknowledgments

This research was funded by UNAM-PAPIIT project IN108914, IN104113 and CONACyT Research Projects 179662. We thank Alexander Knebe for his help with the use of the AHF halo finder and thank Viola Alleinato for the discussion of the values of the HOD, as well as to Vladimir Avila-Reese for helpful comments.

## REFERENCES

- Alexander, D. M., & Hickox, R. C. 2012, *NewAR*, 56, 93  
 Alleinato, V., Finoguenov, A., Cappelluti, N., et al. 2011, *ApJ*, 736, 99  
 Alleinato, V., Finoguenov, A., Hasinger, G., et al. 2012, *ApJ*, 758, 47  
 Arnold, T. J., Martini, P., Mulchaey, J. S., Berti, A., & Jeltema, T. E. 2009, *ApJ*, 707, 1691  
 Barnes, J. E., & Hernquist, L. E. 1991, *ApJ*, 370, L65  
 Barnes, J. E., & Hernquist, L. 1996, *ApJ*, 471, 115  
 Beckmann, V., & Shrader, C. R. 2012, *Active Galactic Nuclei*, ISBN-13: 978-3527410781. 350 pages. Wiley-VCH Verlag GmbH, 2012  
 Behroozi, P. S., Wechsler, R. H., & Conroy, C. 2013, *ApJ*, 770, 57  
 Bonoli, S., Marulli, F., Springel, V., et al. 2009, *MNRAS*, 396, 423

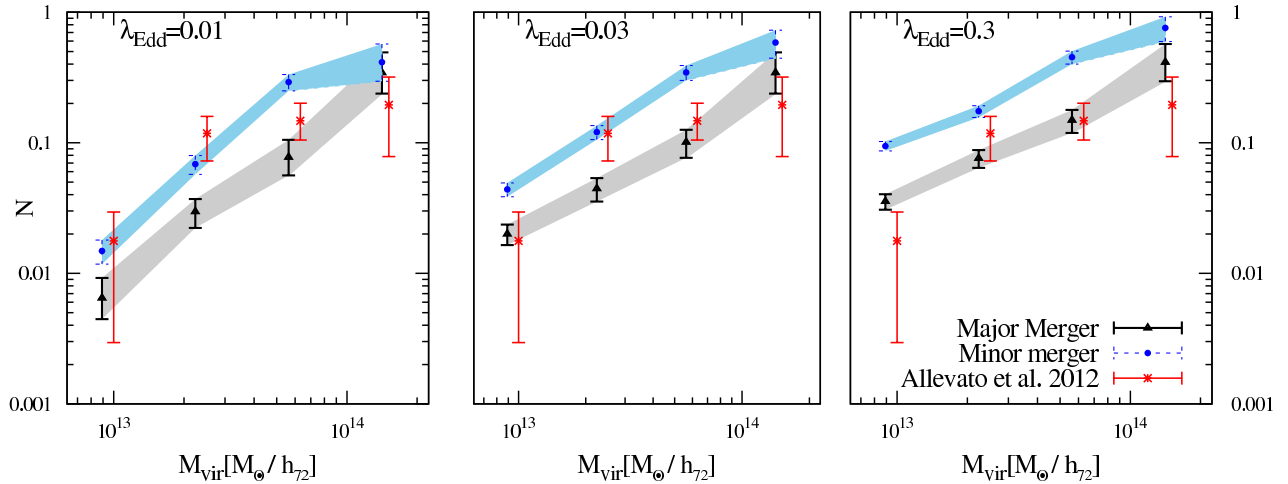


Fig. 3. The HOD of different values of  $\lambda_{Edd}$ , the number of host that harbor a mXAGN triggered by either a major (blue dots) or minor merger (black triangles), and the inferred HOD of satellites mXAGNs by Allevato et al. (2012) (red asterisks).

- Bournaud, F., Dekel, A., Teyssier, R., et al. 2011, *ApJ*, 741, L33
- Cappelluti, N., Allevato, V., & Finoguenov, A. 2012, *Advances in Astronomy*, 2012, 853701
- Ciotti, L., & Ostriker, J. P. 2007, *ApJ*, 665, 1038
- Ciotti, L., Ostriker, J. P., & Proga, D. 2010, *ApJ*, 717, 708
- Cisternas, M., Jahnke, K., Inskip, K. J., et al. 2011, *ApJ*, 726, 57
- Cisternas, M., Gadotti, D. A., Knapen, J. H., et al. 2013, *ApJ*, 776, 50
- Chatterjee, S., Degraf, C., Richardson, J., et al. 2012, *MNRAS*, 419, 2657
- Chatterjee, S., Nguyen, M. L., Myers, A. D., & Zheng, Z. 2013, *ApJ*, 779, 147
- Chen, Y.-M., Wang, J.-M., Yan, C.-S., Hu, C., & Zhang, S. 2009, *ApJ*, 695, L130
- Coil, A. L., Hennawi, J. F., Newman, J. A., Cooper, M. C., & Davis, M. 2007, *ApJ*, 654, 115
- Coil, A. L., Georgakakis, A., Newman, J. A., et al. 2009, *ApJ*, 701, 1484
- Conroy, C., & White, M. 2013, *ApJ*, 762, 70
- Cox, T. J., Jonsson, P., Primack, J. R., & Somerville, R. S. 2006, *MNRAS*, 373, 1013
- Cox, T. J., Dutta, S. N., Hopkins, P. F., & Hernquist, L. 2008, *Panoramic Views of Galaxy Formation and Evolution*, 399, 284
- Crocce, M., Pueblas, S., & Scoccamarro, R. 2006, *MNRAS*, 373, 369
- Croom, S. M., Boyle, B. J., Shanks, T., et al. 2005, *MNRAS*, 356, 415
- Croton, D. J. 2009, *MNRAS*, 394, 1109
- da Ângela, J., Shanks, T., Croom, S. M., et al. 2008, *MNRAS*, 383, 565
- Degraf, C., Di Matteo, T., & Springel, V. 2011, *MNRAS*, 413, 1383
- De Robertis, M. M., Yee, H. K. C., & Hayhoe, K. 1998, *ApJ*, 496, 93
- Di Matteo, P., Combes, F., Melchior, A.-L., & Semelin, B. 2007, *A&A*, 468, 61
- Di Matteo, T., Colberg, J., Springel, V., Hernquist, L., & Sijacki, D. 2008, *ApJ*, 676, 33
- Draper, A. R., & Ballantyne, D. R. 2012, *ApJ*, 753, LL37
- Ebrero, J., Mateos, S., Stewart, G. C., Carrera, F. J., & Watson, M. G. 2009, *A&A*, 500, 749
- Ehlert, S., Allen, S. W., Brandt, W. N., et al. 2015, *MNRAS*, 446, 2709
- Eke, V. R., Frenk, C. S., Baugh, C. M., et al. 2004, *MNRAS*, 355, 769
- Fanidakis, N., Baugh, C. M., Benson, A. J., et al. 2012, *MNRAS*, 419, 2797
- Fanidakis, N., Georgakakis, A., Mountrichas, G., et al. 2013, *MNRAS*, 435, 679
- Farouki, R., & Shapiro, S. L. 1981, *ApJ*, 243, 32
- Gehrels, N. 1986, *ApJ*, 303, 336
- Gebhardt, K., Bender, R., Bower, G., et al. 2000, *ApJ*, 539, L13
- Georgakakis, A., Gerke, B. F., Nandra, K., et al. 2008, *MNRAS*, 391, 183
- Gilmour, R., Best, P., & Almaini, O. 2009, *MNRAS*, 392, 1509
- Gunn, J. E., & Gott, J. R., III 1972, *ApJ*, 176, 1
- Hasinger, G., Miyaji, T., & Schmidt, M. 2005, *A&A*, 441, 417
- Hernquist, L. 1989, *Annals of the New York Academy of Sciences*, 571, 190
- Hernquist, L., & Mihos, J. C. 1995, *ApJ*, 448, 4
- Hopkins, P. F., & Hernquist, L. 2006, *ApJS*, 166, 1
- Hopkins, P. F., Hernquist, L., Cox, T. J., et al. 2006, *ApJS*, 163, 1
- Hopkins, P. F., Lidz, A., Hernquist, L., et al. 2007, *ApJ*, 662, 110
- Hopkins, P. F., Hernquist, L., Cox, T. J., & Kereš, D. 2008, *ApJS*, 175, 356



- Hopkins, P. F., & Hernquist, L. 2009, *ApJ*, 694, 599
- Hopkins, P. F., Bundy, K., Croton, D., et al. 2010, *ApJ*, 715, 202
- Hopkins, P. F., Kocevski, D. D., & Bundy, K. 2014, *MNRAS*, 445, 823
- Jiang, C. Y., Jing, Y. P., & Han, J. 2014, *ApJ*, 790, 7
- Jogee, S. 2006, *Physics of Active Galactic Nuclei at all Scales*, 693, 143
- Kaviraj, S. 2014, *MNRAS*, 440, 2944
- Karouzos, M., Jarvis, M. J., & Bonfield, D. 2014, *MNRAS*, 439, 861
- Kayo, I., & Oguri, M. 2012, *MNRAS*, 424, 1363
- Kendall, P., Magorrian, J., & Pringle, J. E. 2003, *MNRAS*, 346, 1078
- Knebe, A., Knollmann, S. R., Muldrew, S. I., et al. 2011, *MNRAS*, 415, 2293
- Knollmann, S. R., & Knebe, A. 2009, *ApJS*, 182, 608
- Kocevski, D. D., Faber, S. M., Mozena, M., et al. 2012, *ApJ*, 744, 148
- Kormendy, J., & Ho, L. C. 2013, *ARA&A*, 51, 511
- Krumpe, M., Miyaji, T., & Coil, A. L. 2010, *ApJ*, 713, 558
- Krumpe, M., Miyaji, T., Coil, A. L., & Aceves, H. 2012, *ApJ*, 746, 1
- Krumpe, M., Miyaji, T., & Coil, A. L. 2014, *Multifrequency Behaviour of High Energy Cosmic Sources*, 71
- Krumpe, M., Miyaji, T., Husemann, B., et al. 2015, *arXiv:1509.01261*
- Larson, D., Dunkley, J., Hinshaw, G., et al. 2011, *ApJS*, 192, 1
- Leauthaud, A., J. Benson, A., Civano, F., et al. 2015, *MNRAS*, 446, 1874
- Lee, G.-H., Woo, J.-H., Lee, M. G., et al. 2012, *ApJ*, 750, 141
- Lewis, A., Challinor, A., & Lasenby, A. 2000, *ApJ*, 538, 473
- Libeskind, N. I., Yepes, G., Knebe, A., et al. 2010, *MNRAS*, 401, 188
- Lidz, A., Hopkins, P. F., Cox, T. J., Hernquist, L., & Robertson, B. 2006, *ApJ*, 641,
- Lusso, E., Comastri, A., Simmons, B. D., et al. 2012, *MNRAS*, 425, 623
- Makino, J., & Hut, P. 1997, *ApJ*, 481, 83
- Marulli, F., Bonoli, S., Branchini, E., et al. 2009, *MNRAS*, 396, 1404
- Merritt, D., & Ferrarese, L. 2001, *ApJ*, 547, 140
- Mihos, J. C., & Hernquist, L. 1996, *ApJ*, 464, 641
- Milosavljević, M., Merritt, D., & Ho, L. C. 2006, *ApJ*, 652, 120
- Miyaji, T., Zamorani, G., Cappelluti, N., et al. 2007, *ApJS*, 172, 396
- Miyaji, T., Krumpe, M., Coil, A. L., & Aceves, H. 2011, *ApJ*, 726, 83
- Miyaji, T., Hasinger, G., Salvato, M., et al. 2015, *ApJ*, 804, 104
- Mountrichas, G., Sawangwit, U., Shanks, T., et al. 2009, *MNRAS*, 394, 2050
- Mountrichas, G., & Georgakakis, A. 2012, *MNRAS*, 420, 514
- Padmanabhan, N., White, M., Norberg, P., & Porciani, C. 2009, *MNRAS*, 397, 1862
- Porciani, C., Magliocchetti, M., & Norberg, P. 2004, *MNRAS*, 355, 1010
- Pujol, A., & Gaztañaga, E. 2014, *MNRAS*, 442, 1930
- Ramón-Fox, F. G., & Aceves, H. 2014, *Structure and Dynamics of Disk Galaxies*, 480, 229
- Richardson, J., Zheng, Z., Chatterjee, S., Nagai, D., & Shen, Y. 2012, *ApJ*, 755, 30
- Sanders, D. B., Soifer, B. T., Elias, J. H., et al. 1988, *ApJ*, 325, 74
- Schawinski, K., Treister, E., Urry, C. M., et al. 2011, *ApJ*, 727, L31
- Shankar, F., Crocce, M., Miralda-Escudé, J., Fosalba, P., & Weinberg, D. H. 2010, *ApJ*, 718, 231
- Sijacki, D., Springel, V., Di Matteo, T., & Hernquist, L. 2007, *MNRAS*, 380, 87
- Silk, J., & Rees, M. J. 1998, *A&A*, 331, L1
- Silverman, J. D., Miniati, F., Finoguenov, A., et al. 2014, *ApJ*, 780, 67
- Starikova, S., Cool, R., Eisenstein, D., et al. 2011, *ApJ*, 741, 15
- Shen, Y. 2009, *ApJ*, 704, 89
- Shen, Y., Hennawi, J. F., Shankar, F., et al. 2010, *ApJ*, 719, 1693
- Springel, V. 2005, *MNRAS*, 364, 1105
- Springel, V., White, S. D. M., Jenkins, A., et al. 2005, *Nature*, 435, 629
- Springel, V., Di Matteo, T., & Hernquist, L. 2005, *MNRAS*, 361, 776
- Taniguchi, Y. 1999, *ApJ*, 524, 65
- Tapia, T., Eliche-Moral, M. C., Querejeta, M., et al. 2014, *A&A*, 565, AA31
- Thacker, R. J., Scannapieco, E., & Couchman, H. M. P. 2006, *ApJ*, 653, 86
- Thacker, R. J., Scannapieco, E., Couchman, H. M. P., & Richardson, M. 2009, *ApJ*, 693, 552
- Treister, E., Schawinski, K., Urry, C. M., & Simmons, B. D. 2012, *ApJ*, 758, L39
- Tremaine, S., Gebhardt, K., Bender, R., et al. 2002, *ApJ*, 574, 740
- Ueda, Y., Akiyama, M., Ohta, K., & Miyaji, T. 2003, *ApJ*, 598, 886
- Ueda, Y., Akiyama, M., Hasinger, G., Miyaji, T., & Watson, M. G. 2014, *ApJ*, 786, 104
- Van Wassenhove, S., Volonteri, M., Mayer, L., et al. 2012, *ApJ*, 748, LL7
- Villarroel, B., & Korn, A. J. 2014, *Nature Physics*, 10, 417
- Wake, D. A., Croom, S. M., Sadler, E. M., & Johnston, H. M. 2008, *MNRAS*, 391, 167
- Wyithe, J. S. B., & Loeb, A. 2003, *ApJ*, 595, 614
- Wyse, R. F. G. 2004, *ApJ*, 612, L17
- Zavala, J., Avila-Reese, V., Firmani, C., & Boylan-Kolchin, M. 2012, *MNRAS*, 427, 1503
- Zehavi, I., Zheng, Z., Weinberg, D. H., et al. 2011, *ApJ*,

